

# Exploring solutions to the muon $g-2$ anomaly in a 3-3-1 model under flavor constraints

A. Doff<sup>a</sup>, João Paulo Pinheiro<sup>b</sup>, and C. A. de S. Pires<sup>c</sup>

<sup>a</sup> *Universidade Tecnológica Federal do Parana - UTFPR - DAFIS,*

*R. Doutor Washington Subtil Chueire,*

*330 - Jardim Carvalho, 84017-220, Ponta Grossa, PR, Brazil*

<sup>b</sup> *Departament de Física Quàntica i Astrofísica and Institut de Ciències del Cosmos,*

*Universitat de Barcelona, Diagonal 647, E-08028 Barcelona, Spain and*

<sup>c</sup> *Departamento de Física, Universidade Federal da Paraíba,*

*Caixa Postal 5008, 58051-970, João Pessoa, PB, Brazil*

(Dated: January 17, 2025)

## Abstract

The magnetic moment of the muon can receive significant two-loop contributions from a light pseudoscalar. Notably, the spectrum of scalars of 3-3-1 models include one pseudoscalar. However this scalar spectrum inevitably gives rise to flavor-changing neutral current (FCNC) processes. In this study, we examine, within the 3-3-1 model with right-handed neutrinos, whether such spectrum of scalars can account for the anomalous magnetic moment of the muon, considering the constraints imposed by  $B$ -meson decays, meson mixing, and invisible Higgs decays. Our principal finding reveals that a pseudoscalar with mass around 66 GeV and  $\tan\beta = 58$  can account for the  $g - 2$  anomaly without conflicting with flavor physics.

## I. INTRODUCTION

The anomalous magnetic moment of the muon,  $a_\mu \equiv (g_\mu - 2)/2$ , stands amongst the best probes of the Standard Model (SM) of particle physics and its possible extensions. Recently, the Muon  $g-2$  Experiment at Fermilab announced a new experimental (exp) measurement of  $a_\mu$  [1, 2] which, when combined with the previous and consistent results from the same experiment [3–6] (and from the earlier Muon  $g-2$  Experiment at Brookhaven [7–9]), results in a new world average of  $a_\mu^{\text{exp}} = 116592059(22) \times 10^{-11}$  with an unprecedented precision of 190 parts-per-billion (ppb). The standard model prediction, when evaluated using data driven dispersive approach, provides  $a_\mu^{\text{SM}} = 116591810(43) \times 10^{-11}$  [10], which implies in  $\Delta a_\mu \equiv a_\mu^{\text{exp}} - a_\mu^{\text{SM}} = (24.9 \pm 4.8) \times 10^{-10}$ , yielding a discrepancy of  $5.1\sigma^1$ . The explanation of such discrepancy suggests the necessity of new physics beyond the Standard Model (SM). The task of theoretical particle physics is to find scenarios of new physics that provide an explanation to such discrepancy. Generally, any new physics contributing to  $a_\mu$  likely involves hypothetical new particles, including vector or scalar bosons, fermions, or pseudoscalars. Some of these particles may contribute positively to  $a_\mu$ , while others may contribute negatively<sup>2</sup>.

The challenge in resolving the  $a_\mu$  anomaly arises from the difficulty in balancing the positive and negative contributions to align with the observed value of  $a_\mu$ . Among the various new contributions, the one from pseudoscalars is singular because, at the one-loop level, it contributes negatively, whereas at the two-loop level, it contributes positively<sup>3</sup>. Thus, explaining  $a_\mu$  solely with pseudoscalars requires a pseudoscalar with a mass in the tens of GeVs[12, 13]. Consequently, scenarios featuring pseudoscalars that can accommodate  $a_\mu$  are highly motivated for further investigation[13–19].

Models based on the  $SU(3)_C \times SU(3)_L \times U(1)_N$  (3-3-1) symmetry present an intriguing avenue for exploring physics beyond the SM. These models possess a large spectrum of particles contributing to  $a_\mu$ . However the extensive investigation done in Ref. [20] showed that no one version of 3-3-1 models solves the current muon  $g - 2$  anomaly<sup>4</sup>. This finding was based on an energy regime where all the 3-3-1 models belongs to the TeV scale and only single-loop con-

<sup>1</sup>A new  $g - 2$  experiment with a completely different approach is currently under construction at J-PARC[11]

<sup>2</sup>However, it is important to stress that high-precision lattice QCD calculations result in independent, but consistent, values for  $a_\mu$  that are in agreement with  $a_\mu^{\text{exp}}$  and support a no-new-physics in the muon  $g - 2$  scenario[10]

<sup>3</sup>The contribution of charged scalars is negative for one-loop and positive for two-loops too, however (in the discussed scenario) as we will present in the text,  $m_{h^\pm} \geq 483$  GeV, leading to a subdominant contribution (in comparison to A)

<sup>4</sup>The simplest extension of the 3-3-1 model with right-handed neutrinos that explains  $\Delta a_\mu$  at one loop level involves the introduction of a singlet of scalar leptoquark[21]. For <sup>2</sup>other possibilities, see Refs. [20, 22–26]

tributions were considered. The motivation for the current study is to explore the muon  $g - 2$  anomaly within a version of the 3-3-1 models called the 3-3-1 model with right-handed neutrinos (331RHN)[27, 28]. The study will be performed in a regime of energy where some neutral components of the spectrum of scalars of the model, as its intrinsic pseudoscalar, acquire masses at electroweak scale or lower[29] and take into account both one- and -two loop contributions under the constraints of flavor physics.

This work is organized in the follow way: in Sec. II we present the 331RHN and its variants. In the Sec. III we calculate the one- and two-loops contributions to  $\Delta a_\mu$ . In Sec. IV we obtain the theoretical and experimental constraints on the masses of the scalars that contribute to the  $g - 2$ . In Sec. V we present our numerical analysis and in Sec. VI we present a short discussion followed by the main conclusions.

## II. THE 331RHN AND ITS VARIANTS

Our study here is restricted to the 331RHN. Each version of 3-3-1 models dismembers into three variants [30, 31]. In order to understand this, we make a short review how this occurs inside the 331RHN.

In the 331RHN the right-handed neutrinos compose the third components of the triplet of leptons,  $f_{l_L} = (v_{l_L} \ e_{l_L} \ \nu_{l_R}^c)^T$  with  $l = e, \mu, \tau$  representing the three SM generations of leptons.

The gauge sector of the model involves the standard gauge bosons plus one  $Z'$ , two new charged gauge bosons  $W'^{\pm}$  and two non-hermitian neutral gauge bosons  $U^0$  and  $U^{0\prime}$  [32]. All these new gauge bosons must develop mass at TeV scale and due to this their contributions to the  $a_\mu$  are negligible as showed in Ref.[20].

The scalar sector is composed by the three triplets of scalars  $\eta = (\eta^0 \ \eta^- \ \eta'^0)^T$ ,  $\rho = (\rho^+ \ \rho^0 \ \rho'^+)^T$  and  $\chi = (\chi^0 \ \chi^- \ \chi'^0)^T$  with  $\eta$  and  $\chi$  transforming as  $(1, 3, -1/3)$  and  $\rho$  as  $(1, 3, 2/3)$ [33]. After spontaneous breaking of the symmetries, such content of scalar generates masses for all massive particles of the model including fermions and gauge bosons<sup>5</sup>. In order to avoid spontaneous breaking of the lepton number, we assume that only  $\eta^0$ ,  $\rho^0$ , and  $\chi'^0$  develop VEV, namely  $v_\eta, v_\rho, v_{\chi'}$  respectively<sup>6</sup>. The potential, the minimum conditions and the spectrum of scalars of the model are found in Ref. [29]. We just remember here that  $v_\eta^2 + v_\rho^2 = v^2$  where  $v$  is the standard vev whose value

<sup>5</sup>For the development of the other sectors of the model, see Refs.[30, 34–36]

<sup>6</sup>For the case where the other neutral scalars develop VEVs, see Ref. [37]

is 246 GeV. The vev,  $v_{\chi'}$ , characterizes the energy scale of the breaking of the  $SU(3)_L \times U(1)_N$  symmetry. Current LHC bounds impose  $v_{\chi'} \geq 10\text{TeV}$ [38, 39]. Moreover, we remember that the potential of the model involves a trilinear term modulated by the energy parameter  $f$ . This parameter is very important because it regulates the range of values the masses of the spectrum of scalar may achieve. It was showed in Ref. [29] that when  $f < v_\eta, v_\rho$  the range of values of the masses of the scalars may vary from tens of GeVs up to TeV scale. For  $f \geq v_\eta, v_\rho$  all the spectrum of new scalars, except the Higgs, develops mass at  $v_{\chi'}$  scale. Our interest here is exclusively in the first case in which  $f < v_\eta, v_\rho, v_{\chi'}$ . In general the spectrum of scalars of the model is composed by three CP-even scalars  $h_1, h_2$  and  $H$ , two charged scalars  $h_1^+$  and  $h_2^+$ , the pseudo scalar  $A$  and one neutral bilepton  $\eta'^0$ . The scalar  $h_1$  will play the role of the standard-like Higgs. The pseudo scalar  $A$  has mass proportional to the trilinear coupling  $f$ , meaning it may be light if  $f$  is small. What we do here is to investigate the contributions of this set of scalars to the muon  $(g - 2)$  at one and two loops in a general way taking into account the contributions of the gauge bosons of the 331RHN inside the variant of the model that enhance the couplings of the charged leptons with the pseudo scalar  $A$  by means of  $\tan\beta$ . In other words, we complement the job done in Ref. [20].

We remember here that in 331 models anomaly cancellations demand that one family of quarks transforms differently from the other two ones. This feature generates the variants of the models[30]. In what follow we consider the three variants and separate the main aspects of them that matter to the calculation of their contributions to the  $a_\mu$  at one and two loops.

### A. Variant I

In this variant the first two families of quarks transform as anti-triplet while the third one transforms as triplet by  $SU(3)_L$ ,

$$\begin{aligned}
Q_{iL} &= \begin{pmatrix} d_i \\ -u_i \\ d'_i \end{pmatrix}_L \sim (3, \bar{3}, 0), u_{iR} \sim (3, 1, 2/3), \\
d_{iR} &\sim (3, 1, -1/3), \quad d'_{iR} \sim (3, 1, -1/3), \\
Q_{3L} &= \begin{pmatrix} u_3 \\ d_3 \\ u'_3 \end{pmatrix}_L \sim (3, 3, 1/3), u_{3R} \sim (3, 1, 2/3), \\
d_{3R} &\sim (3, 1, -1/3), \quad u'_{3R} \sim (3, 1, 2/3),
\end{aligned} \tag{1}$$

where the index  $i = 1, 2$  is restricted to only two generations. The negative signal in the anti-triplet  $Q_{iL}$  is just to standardise the signals of the charged current interactions with the gauge bosons. The primed quarks are new heavy quarks with the usual  $(+\frac{2}{3}, -\frac{1}{3})$  electric charges.

Here the simplest Yukawa interactions that generate the correct mass for all standard quarks are composed by the terms<sup>7</sup>,

$$-\mathcal{L}_Y \supset g_{ia}^1 \bar{Q}_{iL} \eta^* d_{aR} + h_{3a}^1 \bar{Q}_{3L} \eta u_{aR} + g_{3a}^1 \bar{Q}_{3L} \rho d_{aR} + h_{ia}^1 \bar{Q}_{iL} \rho^* u_{aR} + \text{H.c.}, \quad (2)$$

where  $a = 1, 2, 3$  and the parameters  $g_{ab}^1$  and  $h_{ab}^1$  are Yukawa couplings that, for sake of simplification, we consider reals. Observe that in this variant the dominant term that determines the mass of the quark top involves  $v_\eta$ . Than, in this case, it is natural to assume  $v_\eta > v_\rho$ . With all this in hand, after developing the Yukawa and the scalar sectors as in Refs.[41–43], we present the Yukawa interaction terms that give the main contributions to the  $g - 2$  of the muon at two loops,

$$\begin{aligned} \mathcal{L}_Y = & i \left( -\frac{\tan\beta}{v} (V_L^u)_{i3} (V_L^u)_{3i} + \frac{\cot\beta}{v} (V_L^u)_{33} (V_L^u)_{33} \right) m_i \bar{l} \gamma_5 t A \\ & + i \left( -\frac{\cot\beta}{v} (V_L^d)_{i3} (V_L^d)_{3i} + \frac{\tan\beta}{v} (V_L^d)_{33} (V_L^d)_{33} \right) m_b \bar{b} \gamma_5 b A \\ & + i \frac{tg\beta}{v} m_l \bar{l} \gamma_5 l A \end{aligned} \quad (3)$$

where the subscripts  $i = 1, 2$ . The charged leptons are represented by  $l = e, \mu, \tau$ . The standard vev is  $v = 247\text{GeV}$  and  $V_L^{u,d}$  are the matrices that mix the left handed quarks. Right-handed quarks are assumed in a diagonal basis. In this variant we define  $\tan\beta = \frac{v_\eta}{v_\rho} > 1$ .

<sup>7</sup>For the most general Yukawa interactions involving terms that violate lepton number, see: [40].

## B. Variant II

In this case the first family transforms as triplet and the second and third families transform as anti-triplet, which means

$$\begin{aligned}
Q_{1L} &= \begin{pmatrix} u_1 \\ d_1 \\ u'_1 \end{pmatrix}_L \sim (3, 3, 1/3), u_{1R} \sim (3, 1, 2/3), \\
d_{1R} &\sim (3, 1, -1/3), u'_{1R} \sim (3, 1, 2/3), \\
Q_{iL} &= \begin{pmatrix} d_i \\ -u_i \\ d'_i \end{pmatrix}_L \sim (3, \bar{3}, 0), u_{3R} \sim (3, 1, 2/3), \\
d_{3R} &\sim (3, 1, -1/3), d'_{3R} \sim (3, 1, -1/3),
\end{aligned} \tag{4}$$

where the index  $i = 2, 3$  is restricted to only two generations.

The minimal set of Yukawa interactions that leads to the correct quark masses involves the terms,

$$\begin{aligned}
- \mathcal{L}_Y \supset & g_{1a}^2 \bar{Q}_{1L} \rho d_{aR} + g_{ia}^2 \bar{Q}_{iL} \eta^* d_{aR} \\
& + h_{1a}^2 \bar{Q}_{1L} \eta u_{aR} + h_{ia}^2 \bar{Q}_{iL} \rho^* u_{aR} + \text{H.c.} .
\end{aligned} \tag{5}$$

Observe that in this case the main contribution to the mass of the quark top is determined by the vev  $v_\rho$ . Then in this case we assume  $v_\rho > v_\eta$ .

Following all the previous procedure done in Variant I, we obtain the following Yukawa interactions involving  $A$  and the standard charged fermions that matter to the calculation of the  $g - 2$  of the muon at two loops,

$$\begin{aligned}
\mathcal{L}_Y &= i \left( \frac{\tan \beta}{v} (V_L^u)_{13} (V_L^u)_3 - \frac{\cot \beta}{v} (V_L^u)_{i3} (V_L^u)_{3i} \right) m_i \bar{l} \gamma_5 t A \\
&+ i \left( \frac{\cot \beta}{v} (V_L^d)_{13} (V_L^d)_{31} - \frac{\tan \beta}{v} (V_L^d)_{i3} (V_L^d)_{3i} \right) m_b \bar{b} \gamma_5 b A \\
&+ \frac{i}{v \tan \beta} m_i \bar{l} \gamma_5 l A
\end{aligned} \tag{6}$$

where the subscripts  $i = 2, 3$ . Here we define  $\tan \beta = \frac{v_\rho}{v_\eta} > 1$ .

### C. Variant III

In this case the second family transforms as triplet while the first and third ones transform as anti-triplet

$$\begin{aligned}
Q_{2L} &= \begin{pmatrix} u_2 \\ d_2 \\ u'_2 \end{pmatrix}_L \sim (3, 3, 1/3), u_{2R} \sim (3, 1, 2/3), \\
d_{2R} &\sim (3, 1, -1/3), u'_{2R} \sim (3, 1, 2/3), \\
Q_{iL} &= \begin{pmatrix} d_i \\ -u_i \\ d'_i \end{pmatrix}_L \sim (3, \bar{3}, 0), u_{iR} \sim (3, 1, 2/3), \\
d_{iR} &\sim (3, 1, -1/3), d'_{iR} \sim (3, 1, -1/3),
\end{aligned} \tag{7}$$

where  $i = 1, 3$ .

Here the Yukawa interactions involve the terms

$$\begin{aligned}
- \mathcal{L}_Y &\supset g_{2a}^3 \bar{Q}_{2L} \rho d_{aR} + g_{ia}^3 \bar{Q}_{iL} \eta^* d_{aR} \\
&+ h_{2a}^3 \bar{Q}_{2L} \eta u_{aR} + h_{ia}^3 \bar{Q}_{iL} \rho^* u_{aR} + \text{H.c.},
\end{aligned} \tag{8}$$

where  $i = 1, 3$ .

Following the procedure of Variant I the interactions of the pseudoscalar  $A$  with the standard quarks and leptons that matter to the calculation for the  $g - 2$  of the muon at two loops are given by,

$$\begin{aligned}
\mathcal{L}_Y &= i \left( \frac{\tan \beta}{v} (V_L^u)_{23} (V_L^u)_{32} - \frac{\cot \beta}{v} (V_L^u)_{i3} (V_L^u)_{3i} \right) m_t \bar{l} \gamma_5 t A \\
&+ i \left( \frac{\cot \beta}{v} (V_L^d)_{23} (V_L^d)_{32} - \frac{\tan \beta}{v} (V_L^d)_{i3} (V_L^d)_{3i} \right) m_b \bar{b} \gamma_5 b A \\
&+ i \frac{m_l}{v \tan \beta} \bar{l} \gamma_5 l A
\end{aligned} \tag{9}$$

where  $i = 1, 3$ ,  $v = 247 \text{ GeV}$  and  $V_L^{u,d}$  are the quark mixing matrices. Here we define  $\tan \beta = \frac{v_\rho}{v_\eta} > 1$ .

All this tell us that each variant of the model will lead to different physical results in what concern flavor physics. We stress that the differences among the three variants that matter to muon  $g - 2$  are the Yukawa interactions of  $A$  with the charged leptons  $l$ . In the case of variant II and III these interactions are suppressed by  $\tan \beta$  while in the variant I it is enhanced by  $\tan \beta$ . So

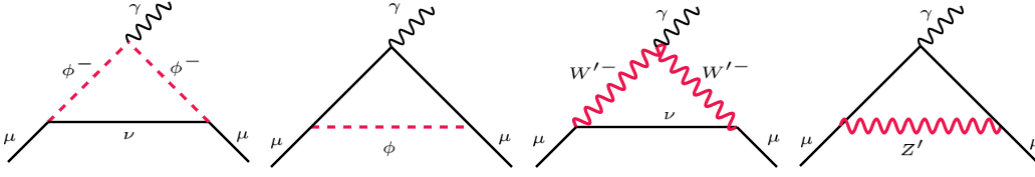


FIG. 1. One-loop contributions to the  $g - 2$  of the muon in the 331RHN where  $\phi$  and  $\phi^-$  represent the neutral and charged scalar contributions

we deduce that only the variant I has potential to explain  $\Delta a_\mu$  at two loops. It is for this reason that from now on we focus exclusively in the variant I of the 331RHN. Observe that we presented the variants involving only the fermions that contribute to  $a_\mu$ . In the APPENDIX we present the general Yukawa interactions involving all the set of scalars for the case of variant I that is the interesting one.

### III. TWO LOOPS CONTRIBUTIONS TO $\Delta a_\mu$ IN THE 331RHN

Before discussing the two loop case, we first review the main aspects of one loop contributions to  $a_\mu$  inside the 331RHN. One loop contributions to the muon anomalous magnetic moment in the 331RHN was extensively investigated in [20]. There it was assumed that  $\tan\beta = 1$  and that the mixing matrices  $V_L^{u,d}$  follow the hierarchy of the CKM one with the main contributions being proportional to  $(V_L^{u,d})_{33}$  which was taken to be  $\approx 1$ . In this case it does not make sense to talk about variants because all the three variants will give the same contributions. In this case the main contributions to  $\Delta a_\mu$  at one loop are due to the new gauge bosons  $W'^{\pm}$  and  $Z'$ , the single charged scalar  $h_1^+$ , the neutral scalar  $h_2$ , and the pseudo scalar  $A$ . The set of interactions and their respective contributions to  $\Delta a_\mu$  are given in Refs. [20, 44]. The Feynman diagrams due to these contributions are showed in FIG. 1.

As it was extensively discussed in Ref.[20], although the 331RHN yields five new contributions at one loop to  $g-2$  with  $W'$  and  $Z'$  giving the dominant positive contributions, unfortunately these five contributions are not able to accommodate the current value of  $a_\mu$  because the negative contributions given by the scalars of the model surpass the positive ones. Thus if we want the 331RHN explains  $\Delta a_\mu$  we need to find positive contributions that surpass the negative ones given at one loop.

It is very well known that  $A$  is responsible for the dominant contribution in two-loops to



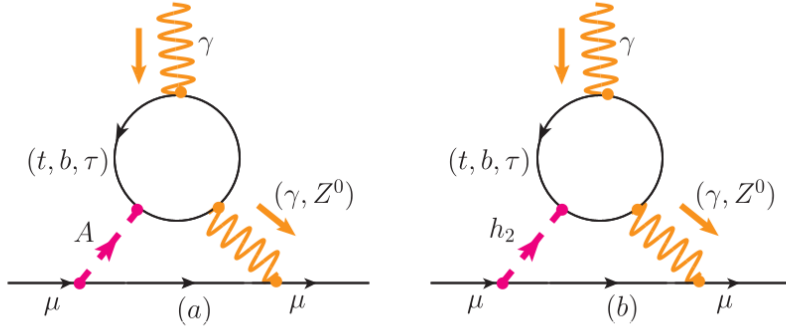


FIG. 2. Two loops Barr-Zee type contributions to the  $g - 2$  of the muon in the 331RHN. In this figure  $h_2$  and  $A$  represent the neutral scalar and pseudoscalar contributions to  $g - 2$  of the muon.

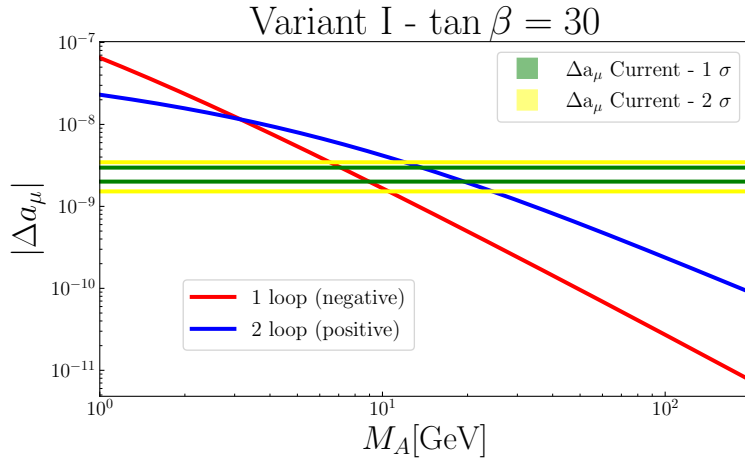


FIG. 3. One and two-loops pseudoscalar contributions for the anomalous  $g-2$  of the muon. The green band represents the actual bounds for the anomaly, the red curve represents the module of the one-loop contribution and the blue curve represents the two-loop contribution of the pseudoscalar  $A$ .

$a_\mu$  [45], [46], [47] and [48]. The 331RHN has a pseudoscalar,  $A$ , in its spectrum of scalars. We then ask for what range of values for  $m_A$  the contributions of the set of scalars ( $h_1$ ,  $h_2$ ,  $h_1^+$ ,  $A$ ) in two loops would accommodate the current value of  $\Delta a_\mu$ . In the two loops, contributions involving  $h_1^+$ ,  $W^{+}$  and  $Z'$  are very suppressed. We neglect them and consider only contributions involving  $A$  and  $h_2$ . We stress that the contribution of  $h_2$ , although small, it is relevant in obtaining the current value of  $\Delta a_\mu$  according to dispersion methods.

Following [46], [47], [48] and [45], we will discuss the contributions to  $a_\mu$  from one and two

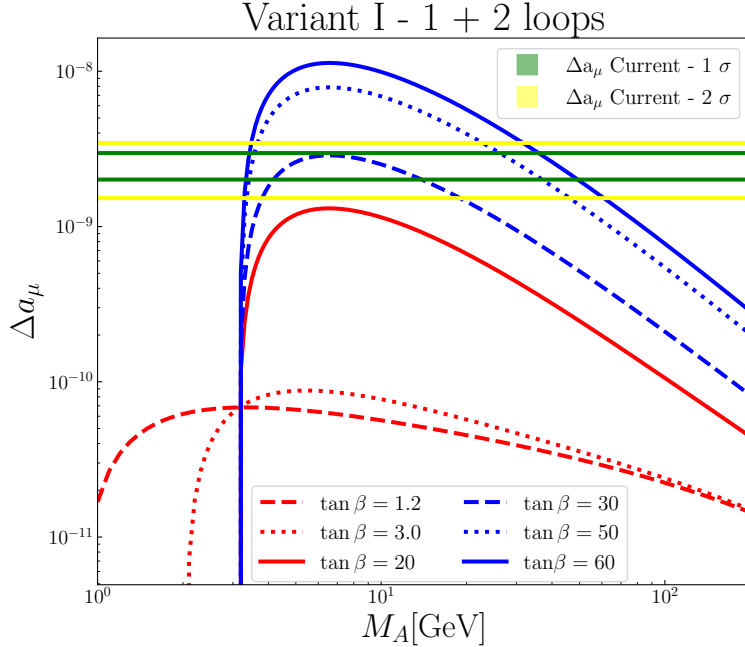


FIG. 4. Here, the curves represents the sum of one and two-loop contributions for the anomalous magnetic moment of the muon for a fixed  $\tan\beta$ . It is clear that, for  $\tan\beta > 27$ , it is always possible to find a point in  $[M_A, \tan\beta]$  plane that explains the  $\Delta a_\mu$ . For more details, see the Appendix.

loops. The expressions for the contributions of one loops are found in Refs. [44] and [20]. For the case of the two loops with  $A$  and  $h_2$  we have two dominant contributions: one involving  $\gamma$  and other involving  $Z$ -boson. The expressions for these contributions are found in Refs. [46], [47] and [48].

In what follow we evaluate such contributions for the variant I of the model as a function of  $M_A$  and  $\tan\beta$ <sup>8</sup>. In FIG. (2) we show the Feynman diagrams of the two loops contributions and in FIG. (3) we present our results for the cases of one and two loops. In that figure the red curve represents the module of the one loop contributions while blue curve represent the two loops contributions due to the pseudo scalar  $A$ , only, that is definitively positive. The green band represents the current bound for the anomaly. The intersection point of the blue and red curves represent the point the two loops contributions cancel the net one loop negative contributions. It occurs at  $M_A \approx 3$  GeVs. From that point ahead the two loops start giving a net positive contribution to  $\Delta a_\mu$ . The intersection point of the blue curve with the green band occurs for  $M_A$  in the range 15 – 25 GeV. Thus the result presented in FIG. (3) tell us that for  $A$  relatively light its two loops contribution

<sup>8</sup>Here we refer to 331RHN because in one loop we consider the main contribution due to  $W'^+$ .

surpasses the negative one loop contributions of the spectrum of 331 model that contributes to muon  $g - 2$  and provides the current  $\Delta a_\mu$ . The value of  $M_A$  in this plot may increase a little as function of  $\tan\beta$ . We show this in FIG. (4) where we present the behaviour of  $\Delta a_\mu$  in function of  $M_A$  for various values of  $\tan\beta$  considering one and two loops contributions. We have that for  $M_A > 3$  GeV and  $\tan\beta > 27$  the 331RHN always offers a point in the plane  $(M_A, \tan\beta)$  that accommodates the current value of  $\Delta a_\mu$ .

However to complete our understanding it is recommended to certify what range of values for  $M_A$  and  $\tan\beta$  accommodates  $\Delta a_\mu$  and respect constraints from flavor physics. More precisely, we must certify the contributions of  $A$  to  $K^0 - \bar{K}^0$  and B mesons decay, in addition to the decay  $h_1 \rightarrow AA$ . We discuss all these constraints right below.

#### IV. THEORETICAL AND EXPERIMENTAL LIMITS

##### A. $K^0 - \bar{K}^0$

In the 331RHN the set of neutral particles  $h_1, h_2, H, A$  and  $Z'$  contribute to FCNC processes<sup>9</sup>. In the scenario where  $A$  solves the muon  $g - 2$  anomaly, where it is the lightest of this set of neutral particles, we must worry with its contribution to FCNC processes as meson transitions. Then it makes mandatory to certify if a pseudoscalar with mass of tens of GeVs is in agreement, for example, with the current value of  $\Delta m_K$  associated to the  $K^0 - \bar{K}^0$  transition. In this regard, the effective Lagrangian that leads to the  $K^0 - \bar{K}^0$  transition can be write as [30]

$$\mathcal{L}_{\text{eff}}^K = -\frac{1}{m_A^2} \left[ \bar{d} \left( C_K^R P_R - C_K^L P_L \right) s \right]^2, \quad (10)$$

where in the equation above  $P_{L,R}$  are the left-handed and right-handed projections. In our case the coefficients  $C_K^{R,L}$  are obtained from the Yukawa interactions given in Eq.(A6) of the APPENDIX. With those interactions we can write

$$\begin{aligned} C_K^R &= \left( \tan\beta (V_L^d)_{32} (V_L^d)_{13} + \cot\beta (V_L^d)_{i2} (V_L^d)_{1i} \right) \frac{m_s}{v} \\ C_K^L &= \left( \tan\beta (V_L^d)_{13}^* (V_L^d)_{32}^* + \cot\beta (V_L^d)_{1i}^* (V_L^d)_{i2}^* \right) \frac{m_d}{v}, \end{aligned} \quad (11)$$

where  $i = 1, 2$ .

<sup>9</sup>For important works treating flavor physics in 331 models, see Refs. [49–54]

With the Lagrangian in Eq.(10), the coefficients in Eq. (11) and following the procedure described in [30], we obtain the following expression to the mixing parameter  $\Delta m_K$  as function of the coefficients  $C_K^{R,L}$

$$\Delta m_K = \frac{2m_K f_k^2}{m_A^2} \left( \frac{5}{24} \text{Re} \left( (C_K^L)^2 + (C_K^R)^2 \right) F^2(k) + 2 \text{Re} \left( C_K^L C_K^R \right) G^2(k) \right), \quad (12)$$

where

$$F^2(k) = \left( \frac{m_K}{m_s + m_d} \right)^2,$$

$$G^2(k) = \left( \frac{1}{24} + \frac{1}{4} F^2(k) \right).$$

In the Eq.(12)  $f_K$  is the kaon( $K^0$ ) decay constant and  $m_k$  is the kaon mass. The input parameters that will be considered in these equations are listed below

$$m_s = 93.4 \text{ MeV}, \quad m_d = 4.67 \text{ MeV}$$

$$m_K = 497.6 \text{ MeV}, \quad f_K = 156 \text{ MeV}.$$

The coefficients  $C_K^{R,L}$  depend on the mixing matrices  $V_L^d$  and  $V_L^u$  whose entries are unknown free parameters that obey the constraint,

$$V_L^u V_L^{d\dagger} = V_{CKM}, \quad (13)$$

which is not sufficient to fix all the entries of  $V_L^{u,d}$ . The pattern of  $V_L^{u,d}$  involves a high level of arbitrariness. A common procedure in works treating meson transitions is to assume aleatory parametrization to the mixing matrix  $V_L^{u,d}$ , see for example Refs. [43, 55–57]. However, it was noted in [31] that once the standard-like Higgs contributes inevitably to meson transitions, too, as it is exposed in the Yukawa interactions in Eq. (A4), and as its contribution depends exclusively of  $V_L^{u,d}$  for fixed angles  $\beta$  and  $\alpha$ , it was then realized that the main role of the Higgs contribution to meson transitions is to auxiliar in the choice of the parametrization of the mixing matrices  $V_L^{u,d}$ .

We then use the following parametrization to the quarks mixing

$$V_L^d \approx \begin{pmatrix} 0.999988 & 0.004863 & -0.0003028 \\ 0.004872 & -0.997974 & 0.0634406 \\ 6.237 \times 10^{-6} & -0.063441 & -0.997974 \end{pmatrix} \quad (14)$$

$$V_L^u \approx \begin{pmatrix} 0.975375 - 2.06267 \times 10^{-8} i & -0.220224 + 0.000209784 i & 0.0127631 + 0.00330004 i \\ -0.22045 - 0.000137853 i & -0.975187 - 6.70389 \times 10^{-7} i & 0.0202181 + 4.17545 \times 10^{-8} i \\ 0.00799242 - 0.00322638 i & -0.0225194 + 0.00072796 i & -0.999704 - 0.0000462961 i \end{pmatrix} \quad (15)$$

In obtaining this parametrization above, following the procedures in Ref. [31], we demanded that the contribution of  $h_1$  to the experimental error of  $\Delta m_K^{\text{exp}}$  is negligible and that the contribution of  $A$  is smaller than the experimental error. This makes of  $V_L^{u,d}$  in Eqs. (14) and Eq. (15) a realistic parametrization for the quark mixing. Throughout this paper we use this parametrization in our calculations.

We are now ready to investigate the effects of a light pseudoscalar,  $A$ , in flavor physics. More precisely, we investigate if the  $K^0 - \bar{K}^0$  transition is compatible with  $M_A \sim (60 - 70)$  GeV's for  $\tan\beta \sim 60$  and the pattern of  $V_L^{u,d}$  given above. We know that the Standard Model contributions to the neutral meson-anti meson transitions present a good agreement with experiments[58–60]. Furthermore, the uncertainty due to errors in QCD corrections must be considered[61, 62]. Therefore, with regard to the contributions from new physics, it is reasonable to consider that these contributions fall inside the experimental error. In the particular case of the  $K^0 - \bar{K}^0$  meson-anti meson transitions we have,

$$\Delta m_K^{\text{exp}} = (3.484 \pm 0.006) \times 10^{-12} \text{ MeV}.$$

Based on these considerations, the experimental errors  $\delta(\Delta m_K)$  of the  $K^0 - \bar{K}^0$  mass difference that we use to constrain new physics is

$$\delta(\Delta m_K) = \pm 0.006 \times 10^{-12} \text{ MeV} = \pm 0.6 \times 10^{-17} \text{ GeV}. \quad (16)$$

Once we demanded that the contribution of  $h_1$  to the error is negligible, we then assume that the contribution of the pseudoscalar  $A$  to the error does not surpass 0.995% of the total error<sup>10</sup>. Note that with respect to the precision used in the parameterization of the matrices (14) and (15), the number of decimal places used in the calculations was maintained in order to obtain the best result for unitarity.

We present our results in FIG. (5) where the blue dashed curve corresponds to the behavior of Eq.(12) with  $M_A$  under the condition that  $\Delta m_K$  stands for 0.995% of the error and for the pattern of quark mixing described by Eq.(14) where  $i, j = 1, 2, 3$ . In that figure the black dotted line corresponds to 0.995% of the error given by Eq.(16) and the dashed red vertical line indicates the position in the band where the pseudoscalar mass,  $M_A = 66$  GeV, explains the  $\Delta a_\mu$  respecting the constraints by flavor changing neutral processes.

<sup>10</sup>We stress here that we are aware that the other neutral particles as  $h_2$  and  $Z'$  also contribute to such error. However as they are much heavier than  $A$ , we think it is reasonable to neglect their contributions to such error[31, 43].

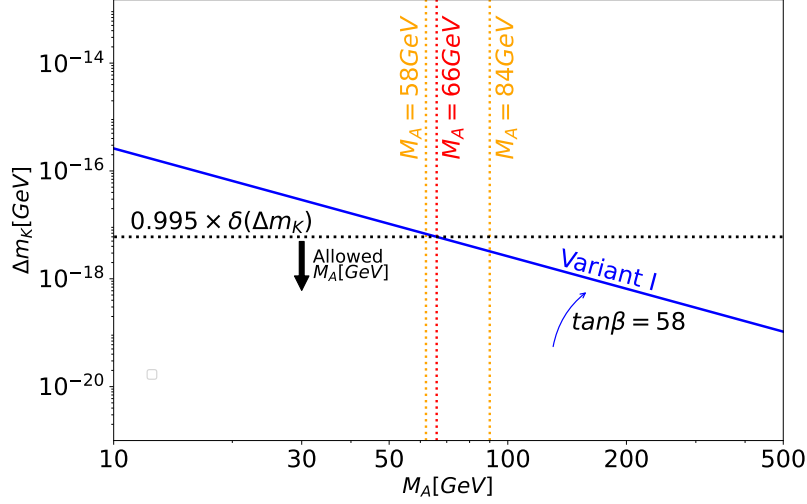


FIG. 5. Flavor changing neutral currents constraint on  $m_A$  from  $K^0 - \bar{K}^0$  transition. We demand  $h_1$  gives negligible contribution to  $\delta(\Delta m_K)$ , and assuming that the contribution of the pseudoscalar  $A$  fall inside the error. The contextualization of the curve behavior is described in the text.

## B. B-meson decays

In this subsection, we will describe important bounds from flavor observables for the 331RHN [63–70].

### 1. $B_s \rightarrow \mu\mu$

The  $B_s \rightarrow \mu\mu$  decay suffer from few hadronic uncertainties and are induced by FCNC transitions, which make them sensitive probes to the effects of physics beyond the SM, especially models with a non-standard Higgs sector. For our particular case, the process is induced by the gauge bosons  $Z, W$  and scalar particles  $A, h_1, h_2$  and  $h_1^\dagger$ . This decay is induced by loop diagrams and any source of FCNC in our theory could in principle contributes to the meson decay. For this analysis, we are using the analytical formulas from [71] and comparing with recent bounds from [72]. One relevant information is that the new vertices that contributes for the diagrams of this decay are proportional to  $\cot\beta$ , meaning that, for  $\tan\beta > 1$ , one expect that, for the studied case, the contribution from new physics would be marginal.

## 2. $B \rightarrow X_s \gamma$

As constantly discussed in the literature, the inclusive radiative decay  $B \rightarrow X_s \gamma$  is one of the most important bounds for the mass of a charged scalar [73–77]. The meson decay is generated by the elemental process  $b \rightarrow s \gamma$  and since the hadron transition occurs in this process, perturbative QCD corrections are much important and non-perturbative effects must be concerned as well. Here, the Higgs scalar particle gives new contributions to the Wilson coefficients of the effective theory. The process is directly proportional to  $\tan \beta$  when  $h_1^+$  is light enough, and this decay figures an important way to bound the mass of the scalar  $h_1^+$ . For sufficiently heavy  $h_1^+$ , the dependence on  $\tan \beta$  vanishes. Then, this bound limits inferiorly the mass of  $h_1^+$ .

The bounds are enhanced after calculating the diagrams for more loops. In the literature, there is analytic calculation for NLO [78]. Recently, a group calculated numerically the NNLO contributions [79] and the constraints on the  $m_{h_1^+}$  parameter are extremely strong ( $> 800$  GeV). However, one important assumption of this paper is that they are not considering FCNC at tree-level. As discussed in the literature [67, 80], on considering models that allows FCNC, the bounds from the inclusive radiative decay imposed on  $m_{h_1^+}$  are relaxed. This is why we are considering in our paper only NLO analytical formulas for the inclusive radiative decay given in [78] and applying the parameterization developed in the  $K - \bar{K}^0$  section. The experimental bounds been used are from [72].

## 3. $B \rightarrow \tau \nu$

Typically there are decay processes like  $M^\pm \rightarrow \ell \nu_\ell$  mediated by the charged scalar. They occur at tree-level and the most relevant bounds comes from the decays  $B \rightarrow \tau \nu$ ,  $D \rightarrow \mu \nu$ ,  $D_s \rightarrow \tau \nu$  and  $D \rightarrow \nu \mu$ . For the considered case in this article, the strongest contribution is given by the process  $B \rightarrow \tau \nu$ , and it is very important to obtain a superior limit for  $\tan \beta$  at different  $h_1^+$  masses. We performed the analysis applying the experimental limits from [72] at 95% C.L. and the analytical formula from [78].

### C. Higgs decay

Concerning the Higgs decay, the interaction  $\mathcal{L}^{hAA} \supset \frac{1}{2}g_{AAh}h_1AA$  allows the decay mode  $h_1 \rightarrow A + A$  when  $m_A < m_h/2$ . If this is the case, we get

$$\Gamma(h_1 \rightarrow AA) = \frac{g_{hAA}^2}{32\pi m_h} \sqrt{1 - \frac{4m_A^2}{m_{h_1}^2}} \quad \text{where} \quad g_{AAh} = \frac{2v(2\lambda_6(\tan^4\beta + 1) + (\lambda_2 + \lambda_3)\tan^2\beta)}{(\tan^2\beta + 1)^2}.$$

This decay enters in the mode invisible of  $h_1$ . For large values of  $\tan\beta$  we have  $g_{hAA} \rightarrow 4\lambda_6v$ . Here  $\lambda_6$  is a function of the mass of the scalars,

$$\lambda_6 = \frac{m_{h_1}^2}{v^2} - \frac{m_{h_2}^2 - 4M_A^2 \cot\beta}{v^2}, \quad (17)$$

and in order to avoid the bounds from the invisible decays of the Higgs, one must artificially reduce the size of  $\lambda_6$  to be nearly zero or imposes  $m_{h_1} = m_{h_2}$  when  $\cot\beta \rightarrow 0$ . However, without fine tuning the only way to escape from this bound is to impose an inferior limit for  $M_A > \frac{m_h}{2}$ . Thus we have to explain  $\Delta a_\mu$  with  $A$  respecting this bound.

### D. Instability conditions

Here we obtain the range of values for the parameters  $[M_A, m_{h_1^\pm}]$  allowed by the stability conditions of the potential[81]. For this we use the most general potential of the 331RHN that conserves lepton number which is given in [82]. In order to avoid spontaneous breaking of the lepton number, it is assumed that only  $\eta^0, \rho^0$ , and  $\chi'^0$  develop VEV<sup>11</sup>. After diagonalizing the the mass matrices of the scalars of the model, we obtain the tree-level scalars masses[29]:

$$M_A^2 = \frac{fv_{\chi'}}{4} \left( \frac{\tan\beta}{1 + \tan\beta^2} \frac{v^2}{v_{\chi'}} + \tan\beta + \cot\beta \right), \quad m_{h_1^\pm}^2 = \frac{1}{2} (fv_{\chi'} + \lambda_9 \frac{\tan\beta}{1 + \tan\beta^2} v^2) (\tan\beta + \cot\beta) \quad (18)$$

These mass expressions and all the other ones are found in [29].

For the decoupling limit of the heavy 331 particles which means to take  $v_{\chi'} \geq 10$  TeV, the phenomenological viable set of scalars are a mixing of  $\rho$  and  $\eta$ . After the decoupling, the relevant bounds from below conditions [83] are expressed by the set of relations

$$\lambda_2 > 0, \quad \lambda_3 > 0, \quad \lambda_6 + 2\sqrt{\lambda_2\lambda_3} > 0, \quad \lambda_6 + \lambda_9 + 2\sqrt{\lambda_2\lambda_3} > 0, \quad (19)$$

while the unitarity and perturbativity conditions [84] are given by  $|\lambda_i| < 4\pi$ .

<sup>11</sup>For the case where the other neutral scalars develop VEVs, see Ref. [40]



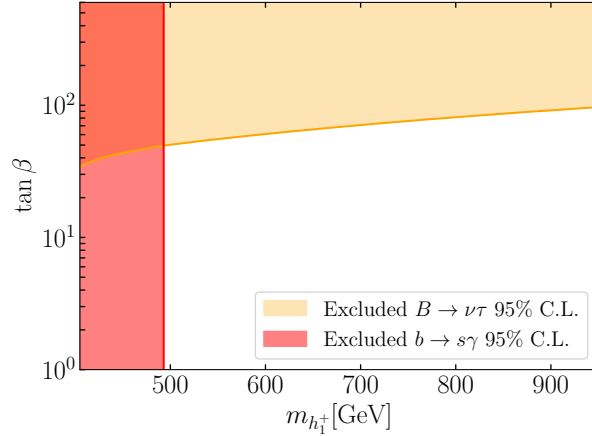


FIG. 6. Excluded regions due to  $B$ -meson decays at 95 % C.L. in the  $[m_{h_1^+}, \tan\beta]$  plane. From these bounds, we projected these bounds into the  $M_A, \tan\beta$  plane without assuming mass degenerescence between  $h_1^+$  and  $A$ .

## V. NUMERICAL ANALYSIS

In this section, we perform a numerical scan in the parameter space of the Variant I of the 331RHN. Here, we are assuming the limit  $v_\chi \gg v_\eta, v_\rho$ . This means that, in addition to the SM particles, there are only three new particles,  $h_2, h_1^\pm$  and  $A$ . We identify  $h_1$  as the standard Higgs and we are considering the alignment limit for the CP-even scalars [85, 86]. For fixed  $v_\chi = 10$  TeV and  $v = 246$  GeV, and adopting the physical basis for the scalar potential in the 331RHN, there are 4 remaining free parameters that we assume varying in the following range:

$$\{\tan\beta \in [1, 200], m_{h_2} \in [5, 1000] \text{ GeV}, M_A \in [5, 1000] \text{ GeV}, m_{h_1^+} \in [100, 1000] \text{ GeV}\}.$$

In FIG. 6, we present the constraints from the processes  $B \rightarrow X_s\gamma$  and  $B \rightarrow \tau\nu$  in the plane  $[m_{h_1^+}, \tan\beta]$ . It is clear in that figure that  $m_{h_1^+}$  is bounded from below independently from the value of  $\tan\beta$ , for  $\tan\beta > 1$

$$m_{h_1^+} > 483 \text{ GeV},$$

while  $B \rightarrow \tau\nu$  limits superiorly the value of  $\tan\beta$ .

After applying the bounds on the plane  $[m_{h_1^+}, \tan\beta]$ , one must project these bounds on the  $[M_A, \tan\beta]$  plane. But first, we will project the flavor bounds into the  $[M_A, m_{h_1^+}]$  plane. This is what is done in FIG. 7. Here, we show the effect of the cumulative bounds from flavor observables in the  $[M_A, m_{h_1^+}]$  plane where the blue dots represents the allowed regions after applying the potential

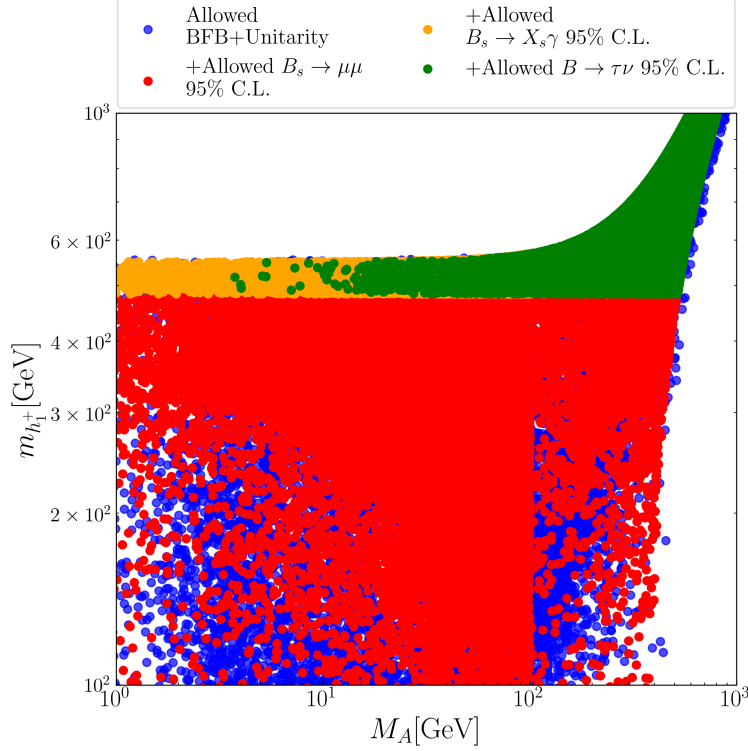


FIG. 7. Here, we can see the relation between the masses of the charged scalar  $h_1^+$  and the pseudoscalar  $A$ . The blue dots represents the possible values for masses in the  $[M_A, m_{h_1^+}]$  plane in which the potential bounds are obeyed (bounded from below conditions and imposing that the mass of all scalars are positive), red dots represents the cumulative bounds from the muon decays of  $B_s$  meson and potential conditions, the yellow dots represents the simultaneous bounds for the decay of  $B_s$  into  $X_s \gamma$  and previous bounds and the green dots represents the cumulative bounds for the decay of  $B$  into  $\tau \nu$  and the previous bounds. All flavor observables at 95% C.L..

bounds (bounded from below conditions (BFB) and unitarity). One interesting fact is that, for high values of  $m_{h_1^+}$ ,  $M_A$  is almost degenerated with it. Then, it is impossible to have light  $A$  when  $h_1^+$  is a heavy particle due the conditions of the potential. This shows how important are the limits from  $B \rightarrow X_s \gamma$ . For the same figure, we cumulatively added the bounds from the  $B_s \rightarrow \mu \mu$  decay. These bounds are represented by red dots. It was discussed in reference [41] that, for  $\tan \beta > 1$ , the influence of  $B_s \rightarrow \mu \mu$  is marginal. However, one can observe that such statement is not exactly true, there is a non-trivial effect for simultaneous light  $m_{h_1^+}$  and  $M_A$ . The orange dots represents the previous cumulative bounds together with the allowed region of the inclusive radiative decay  $B_s \rightarrow X_s \gamma$ . Here it is clear that such bound constrain inferiorly the value of  $m_{h_1^+}$ , however, it still

allows  $M_A$  to be small. The green dots represents the previous cumulative bounds together with the allowed region of the tree-level decay  $B \rightarrow \tau\nu$ . Here, the bound constrains inferiorly the value of  $M_A$  and superiorly the value of  $\tan\beta$ .

In FIG. 8, we projected the discussed bounds from  $h_1^+$  into the  $[M_A, \tan\beta]$  plane. Here, we considered the region that explains the anomalous magnetic moment of the muon for one (two)  $\sigma$  as the green(yellow) contours. At the same time, as discussed in a previous section, we imposed the bounds from the invisible decay of the Higgs into two  $A$ 's. Such bound imposes that  $M_A > 62.5$  GeV, independently from the value of  $\tan\beta$ . After applying all discussed bounds, we discovered a small allowed region that explains the anomalous  $g - 2$  and at the same time obeys all main flavor constraints and do not contribute for the Higgs invisible decay.

Then, we can summarize what we did as:

1. For every point in the  $[M_A, \tan\beta]$  plane, it is possible to find a parametrization for  $V_L^d$  and  $V_L^u$  that avoid the constraints from neutral meson-antimeson transitions  $K^0 - \bar{K}^0$ . Assuming  $M_A = 66$  GeV and  $\tan\beta = 58$  as a benchmark point, we showed the numerical values of the unitary matrices  $V_L^d$  and  $V_L^u$ ;

2. The constraints from  $B_s \rightarrow \mu\mu$  are not relevant for the Variant I, when  $\tan\beta > 1$ , if we simultaneous use bounds from inclusive radiative decay  $b \rightarrow s\gamma$ ;

3. The constraint from  $B \rightarrow X_s\gamma$  depend strongly if you consider FCNC. As we discussed, we found the bound:

$$m_{h_1^+} > 483 \text{ GeV},$$

fixing the values of  $V_L^d$  and  $V_L^u$  as described in the text.

4. The tree-level decay of  $B \rightarrow \tau\nu$  via charged-scalar exchange limits superiorly the value of  $\tan\beta$  and gives an important bound for the plane  $[M_A, \tan\beta]$ . Increasing the precision of this decay is vital to rule out or not the capability of  $A$  to explain the  $g - 2$  anomaly and run away from flavour constraints;

5. There is a small window for  $(g - 2)_\mu$  be explained in the Variant I. The possible solution for the muon  $g - 2$  anomaly that avoids flavor constraints and higgs invisible decay lies on the range  $M_A \in [62.5, 122]$  GeV for  $\tan\beta \in [43, 59]$ ;

6. In order to understand the role of  $h_2$  in the calculation of  $g - 2$  one needs to explore the features of the spectrum of CP-even scalars related to the mass matrix in Eq. (5) of [29]. For this, we solved it numerically, scanning the parameter space as described in the beginning of this section, for tiny  $f$  and  $v_\eta \geq v_\rho$  while demanding  $h_1$  is the 125 GeV Higgs of the standard model.

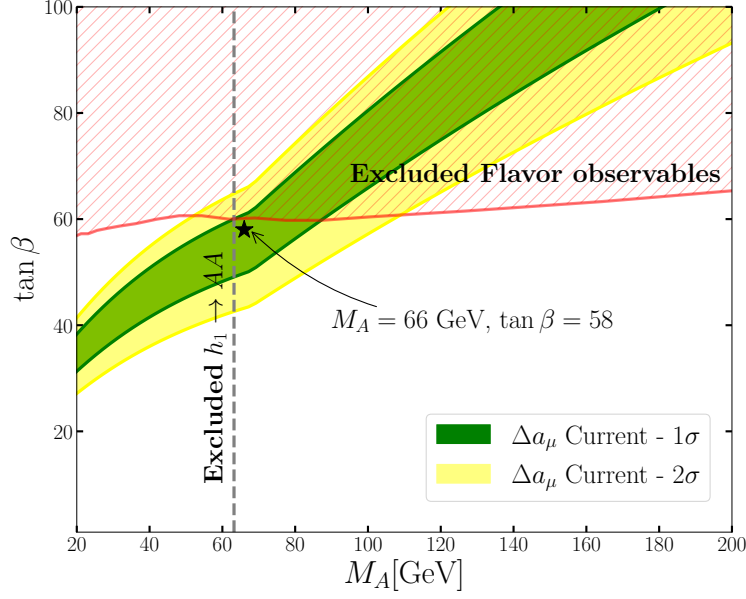


FIG. 8. Imposition of  $B$ -physics bounds into the plane  $[M_A, \tan\beta]$ . The red hatched contour represents the cumulative bounds from the most stringent  $B$ -meson decays to limit parameter space of the pseudoscalar  $A$ ,  $B_s \rightarrow X_s \gamma + B_s \rightarrow \mu\mu + B \rightarrow \tau\nu$  at 95% C.L.. The green(yellow) band represents the current bounds from the anomalous magnetic moment of the muon for 1(2) $\sigma$ . The black star represents one benchmark point that respects the  $B$ -physics bounds, the bounds from the invisible decay of the Higgs and explains the  $\Delta a_\mu$  in the  $[M_A, \tan\beta]$  plane.

For  $\tan\beta < 10$  there is no surprise. However, when  $\tan\beta > 10$  we observed a novelty exclusively for the 3-3-1 scalar potential described in [29]. We observed that for  $M_A > \frac{m_{h_1}}{2}$  the scan gives  $M_A \approx m_{h_2}$ . This is an exclusive feature of the 3-3-1. Concerning the region where  $M_A < \frac{m_{h_1}}{2}$ , given the flexibility to select multiple points in the scan, we have freedom to choose the mass of  $h_2$  to be larger than the half of the Standard Higgs mass. This ensure that  $h_1$  will never decay into two  $h_2$  particles.

As a final comment, one benchmark point that represents the marked star in FIG. 8 is:  $m_{h_1} = 125$  GeV,  $m_{h_2} = 64$  GeV,  $m_{h^+} = 540$  GeV,  $f = 2.96 \times 10^{-2}$  GeV,  $\lambda_1 = 12.5$ ,  $\lambda_2 = 0.85$ ,  $\lambda_3 = -6.89$ ,  $\lambda_4 = 3.38$ ,  $\lambda_5 = -2.06$ ,  $\lambda_6 = -2.24$ ,  $\lambda_9 = 9.34$ .

## VI. DISCUSSION AND CONCLUSION

Explaining the current muon ( $g-2$ ) anomaly using scalar fields remains a significant challenge. At one-loop levels, charged scalars and pseudoscalars typically contribute negatively, whereas CP-even scalars contribute positively. At two-loop levels, however, all these scalars contribute positively. Individually, each scalar could potentially explain the ( $g-2$ ) anomaly, but they must be relatively light, which is particularly challenging for charged scalars. Neutral scalars, especially pseudoscalars, are viable candidates as they can be lighter—albeit heavier than  $\frac{m_{h_1}}{2}$  to avoid invisible Higgs decays—making them natural candidates to address the ( $g-2$ ) anomaly.

Pseudoscalar naturally emerges in 331 model with right-handed neutrinos (331RHN). In regimes where the 331RHN features a light pseudoscalar, there exists a parameter window where a pseudoscalar mass ranging from 62.5 to 120 GeV, combined with a high  $\tan\beta$ , may explain the muon anomaly. We stress here that in the regime where the pseudoscalar accommodate the  $g-2$  results in the CP-even  $h_2$  being degenerate in mass with the pseudoscalar  $A$ . Conversely: the scenario proposed here may be discarded if a second Higgs, heavier than the standard one, is discovered.

Moreover, this model introduces arbitrariness regarding quark mixing, as the parametrization pattern of  $V_L^{u,d}$  cannot be uniquely determined. It is plausible that a suitable parametrization of  $V_L^{u,d}$  could allow heavier pseudoscalars as a solution to the ( $g-2$ ) anomaly, particularly if right-handed quark mixing is considered<sup>12</sup>. Thus, the choice of quark mixing pattern significantly influences all flavor physics processes involving scalars, and determining this pattern is crucial for advancing the field and achieving conclusive results in flavor physics.

In conclusion, the 331RHN model with right-handed neutrinos explain the muon ( $g-2$ ) anomaly through dominant two-loop contributions from a pseudoscalar with a mass in the tens of GeV range and a high  $\tan\beta$ , under the constraints of flavor physics. This position the 331RHN as a compelling framework for exploring new physics beyond the Standard Model.

## ACKNOWLEDGMENTS

We thank A. Cherchiglia for valuable discussions. C.A.S.P was supported by the CNPq research grants No. 311936/2021-0. J. P. P. has received support from the European Union's Hori-

---

<sup>12</sup>Paper in progress.

zon 2020 research and innovation program under the Marie Skłodowska-Curie grant agreement No 860881-HIDDeN.

### Appendix A: One-loop contribution

In this work we follow the spectrum of scalars obtained in Ref. [29] where

$$\begin{aligned} A &= \cos\beta I_\eta + \sin\beta I_\rho, \\ h_1^+ &= \sin\beta\rho^+ + \cos\beta\eta^+ \\ h_2^+ &\approx \rho'^+, \end{aligned} \quad (\text{A1})$$

where  $\cos\beta = \frac{v_\rho}{\sqrt{v_\eta^2+v_\rho^2}}$  and  $\sin\beta = \frac{v_\eta}{\sqrt{v_\eta^2+v_\rho^2}}$ .

For the case of the variant I, we have the following Yukawa interactions among  $h_1^+$  and the quarks

$$\begin{aligned} \mathcal{L} \supset & \sqrt{2}h_1^+ \left( -\frac{\cot\beta}{v}(V_L^d)_{ia}(V_L^u)_{bi} + \frac{\tan\beta}{v}(V_L^d)_{3a}(V_L^u)_{b3} \right) (m_{down})_a \tilde{u}_{bL} \hat{d}_{aR} \\ & + \sqrt{2}h_1^- \left( -\frac{\tan\beta}{v}(V_L^u)_{ia}(V_L^d)_{bi} + \frac{\cot\beta}{v}(V_L^u)_{3a}(V_L^d)_{b3} \right) (m_{up})_a \tilde{d}_{bL} \hat{u}_{aR} + H.c. \end{aligned} \quad (\text{A2})$$

where the subscripts  $i = 1, 2$  and  $a, b = 1, 2, 3$  with  $(m_{down})_{1,2,3} = (m_d, m_s, m_b)$  and  $(m_{up})_{1,2,3} = (m_u, m_c, m_t)$ . The fields  $\hat{u}_{L,R} = (u_{L,R}, c_{L,R}, t_{L,R})$  and  $\hat{d}_{L,R} = (d_{L,R}, s_{L,R}, b_{L,R})$ . Assuming the expression above and Eqs.(14) and (15), the effective Yukawa  $y_{h_1^+}^t$  coupling of the quark top with  $h_1^+$  can be written as

$$y_{h_1^+}^t = 0.004 \tan\beta \frac{m_t}{v} \approx 0.163 \quad (\text{A3})$$

Yukawa interactions with the higgses  $h_1$  and  $h_2$

$$\begin{aligned} \mathcal{L} \supset & \frac{\sqrt{1+\tan\beta^2}}{\tan\beta v} \left[ c_\alpha (V_L^d)_{ia}(V_L^d)_{bi} + s_\alpha \tan\beta (V_L^d)_{3a}(V_L^d)_{b3} \right] (m_{down})_a \tilde{d}_{bL} \hat{d}_{aR} h_1 \\ & + \frac{\sqrt{1+\tan\beta^2}}{\tan\beta v} \left[ s_\alpha \tan\beta (V_L^u)_{ia}(V_L^u)_{bi} + c_\alpha (V_L^u)_{3a}(V_L^u)_{b3} \right] (m_{up})_a \tilde{u}_{bL} \hat{u}_{aR} h_1 + H.c, \end{aligned} \quad (\text{A4})$$

and

$$\begin{aligned} \mathcal{L} \supset & \frac{\sqrt{1+\tan\beta^2}}{\tan\beta v} \left[ -s_\alpha (V_L^d)_{ia}(V_L^d)_{bi} + c_\alpha \tan\beta (V_L^d)_{3a}(V_L^d)_{b3} \right] (m_{down})_a \tilde{d}_{bL} \hat{d}_{aR} h_2 \\ & + \frac{\sqrt{1+\tan\beta^2}}{\tan\beta v} \left[ -c_\alpha \tan\beta (V_L^u)_{ia}(V_L^u)_{bi} - s_\alpha (V_L^u)_{3a}(V_L^u)_{b3} \right] (m_{up})_a \tilde{u}_{bL} \hat{u}_{aR} h_2 + H.c. \end{aligned} \quad (\text{A5})$$

where  $s_\alpha = \sin \alpha$  and  $c_\alpha = \cos \alpha$  are the mixing angle among the neutral higgses  $R_\eta$  and  $R_\rho$  that compose  $h_1$  and  $h_2$  following Ref. [29]

The Yukawa interactions with  $A$  is given by

$$\begin{aligned} \mathcal{L}_Y^A = & iA\tilde{u}_{bL} \left( -\frac{\tan\beta}{v}(V_L^u)_{ia}(V_L^u)_{bi}(m_{up})_a + \frac{\cot\beta}{v}(V_L^u)_{3a}(V_L^u)_{b3}(m_{up})_a \right) \hat{u}_{aR} \\ & + iA\tilde{d}_{bL} \left( \frac{\cot\beta}{v}(V_L^d)_{ia}(V_L^d)_{bi}(m_{down})_a + \frac{\tan\beta}{v}(V_L^d)_{3a}(V_L^d)_{b3}(m_{down})_a \right) \hat{d}_{aR} + \text{H.c.}, \end{aligned} \quad (\text{A6})$$

the indexes  $i = 1, 2$  and  $a, b = 1, 2, 3$  were defined in the previous expressions. Considering the expression above and Eqs.(14) and (15), the effective Yukawa  $y_A^t$  coupling of the quark top with  $A$  can be written as

$$y_A^t = 0.004 \tan\beta \frac{m_t}{v} \approx 0.163. \quad (\text{A7})$$

### Appendix B: One and two-loop contribution of CP-odd scalar

The light CP-odd scalars negative one-loop contribution for the anomalous magnetic moment of the muon is given by:

$$\Delta a_\mu(A)^{(1\text{-loop})} = -\frac{m_\mu^2}{8\pi^2 M_A^2} \left( \frac{g^2 m_\mu^2 A_\mu^2}{4M_W^2} \right) H\left(\frac{m_\mu^2}{M_A^2}\right), \quad (\text{B1})$$

such that  $H(y) = \int_0^1 \frac{x^3 dx}{1-x+x^2 y}$ . The light CP-odd scalars positive two-loop contribution for the anomalous magnetic moment of the muon is given by:

$$\Delta a_\mu(A)^{(2\text{-loop})} = \Delta a_\mu(A)_\gamma^{(2\text{-loop})} + \Delta a_\mu(A)_Z^{(2\text{-loop})}, \quad (\text{B2})$$

such that:

$$\Delta a_\mu(A)_\gamma^{(2\text{-loop})} = \frac{\alpha^2}{8\pi^2 \sin^2 \theta_W} \frac{m_\mu^2 A_\mu}{M_W^2} \sum_{f=t,b,\tau} N_c^f q_f^2 A_f \frac{m_f^2}{M_A^2} \mathcal{F}\left(\frac{m_f^2}{M_A^2}\right) \quad (\text{B3})$$

and

$$\Delta a_\mu(A)_Z^{(2\text{-loop})} = \frac{\alpha^2 m_\mu^2 A_\mu g_V^\mu}{8\pi^2 \sin^4 \theta_W \cos^4 \theta_W M_Z^2} \sum_{f=t,b,\tau} \frac{N_c^f g_V^f q_f A_f m_f^2}{M_Z^2 - M_A^2} \left[ \mathcal{F}\left(\frac{m_f^2}{M_Z^2}\right) - \mathcal{F}\left(\frac{m_f^2}{M_A^2}\right) \right] \quad (\text{B4})$$

such that  $g_V^f = \frac{1}{2}T_3(f_L) - q_f \sin^2 \theta_W$  and  $\mathcal{F}(x) = \int_0^1 dz \ln\left(\frac{x}{z(1-z)}\right) \frac{1}{x-z(1-z)}$ .

We performed the full calculation using the analytical formulas from [47], adding charged and CP-even scalars too.

### Appendix C: Asymptotic Limits

Analyzing FIG. 4, it is possible to observe, for sufficiently high values of  $\tan\beta$ , a particular value of  $M_A$  in which the 2-loop contribution for the  $g - 2$  of the muon becomes dominant in relation to the 1-loop one.

Here in this appendix, we will try to estimate analytically which value of  $M_A$  the two-loop contribution becomes dominant. One first observation is that  $\Delta a_\mu(A)_Z^{(2\text{-loop})}$  is always suppressed in relation to  $\Delta a_\mu(A)_\gamma^{(2\text{-loop})}$ . Then, it is sufficient to understand the limit in which the photon Barr-Zee contribution is larger than the negative one-loop contribution, or,  $\Delta a_\mu(A)_\gamma^{(2\text{-loop})} + \Delta a_\mu(A)^{(1\text{-loop})} = 0$ .

Using equations B1 and B3, we will obtain the approximated equation:

$$\frac{1}{3}m_b^2\mathcal{F}\left(\frac{m_b^2}{M_A}\right) + \frac{4}{3\tan^4\beta}m_t^2\ln\left(\frac{m_t^2}{M_A^2}\right) + m_\tau^2\mathcal{F}\left(\frac{m_\tau^2}{M_A}\right) = \frac{g^2s_W^2m_\mu^2}{4\alpha^2}H\left(\frac{m_\mu^2}{M_A^2}\right) \quad (\text{C1})$$

For  $\tan\beta$  larger than one and smaller than 5, the top-quark contribution is relevant to the total magnetic moment of the muon. However, for such small values of  $\tan\beta$ , it is not possible for  $A$  to explain the anomaly(FIG. 4). For  $\tan\beta > 5$ , the top-quark contribution is irrelevant to the total magnetic moment of the muon. Not only that,  $\Delta a_\mu(A)_\gamma^{(2\text{-loop})} = -\Delta a_\mu(A)^{(1\text{-loop})}$  becomes independent of  $\tan\beta$ , as observed in FIG. 4, too.

Now, solving numerically:

$$\frac{1}{3}m_b^2\mathcal{F}\left(\frac{m_b^2}{M_A}\right) + m_\tau^2\mathcal{F}\left(\frac{m_\tau^2}{M_A}\right) = \frac{g^2s_W^2m_\mu^2}{4\alpha^2}H\left(\frac{m_\mu^2}{M_A^2}\right) \quad (\text{C2})$$

leads to  $M_A \approx 3.16$  GeV, explaining the shape of the figures in FIG. 4.

- 
- [1] D. P. Aguillard et al. (Muon  $g-2$ ), *Phys. Rev. Lett.* **131**, 161802 (2023), [arXiv:2308.06230 \[hep-ex\]](#).
  - [2] D. P. Aguillard et al. (Muon  $g-2$ ), (2024), [arXiv:2402.15410 \[hep-ex\]](#).
  - [3] B. Abi et al. (Muon  $g-2$ ), *Phys. Rev. Lett.* **126**, 141801 (2021), [arXiv:2104.03281 \[hep-ex\]](#).
  - [4] T. Albahri et al. (Muon  $g-2$ ), *Phys. Rev. Accel. Beams* **24**, 044002 (2021), [arXiv:2104.03240 \[physics.acc-ph\]](#).
  - [5] T. Albahri et al. (Muon  $g-2$ ), *Phys. Rev. A* **103**, 042208 (2021), [arXiv:2104.03201 \[hep-ex\]](#).
  - [6] T. Albahri et al. (Muon  $g-2$ ), *Phys. Rev. D* **103**, 072002 (2021), [arXiv:2104.03247 \[hep-ex\]](#).
  - [7] G. W. Bennett et al. (Muon  $g-2$ ), *Phys. Rev. D* **73**, 072003 (2006), [arXiv:hep-ex/0602035](#).



- [8] G. W. Bennett *et al.* (Muon  $g-2$ ), *Phys. Rev. Lett.* **89**, 101804 (2002), [Erratum: *Phys.Rev.Lett.* 89, 129903 (2002)], [arXiv:hep-ex/0208001](#).
- [9] G. W. Bennett *et al.* (Muon  $g-2$ ), *Phys. Rev. Lett.* **92**, 161802 (2004), [arXiv:hep-ex/0401008](#).
- [10] T. Aoyama *et al.*, *Phys. Rept.* **887**, 1 (2020), [arXiv:2006.04822 \[hep-ph\]](#).
- [11] M. Abe *et al.*, *PTEP* **2019**, 053C02 (2019), [arXiv:1901.03047 \[physics.ins-det\]](#).
- [12] A. Broggio, E. J. Chun, M. Passera, K. M. Patel, and S. K. Vempati, *JHEP* **11**, 058 (2014), [arXiv:1409.3199 \[hep-ph\]](#).
- [13] T. Han, S. K. Kang, and J. Sayre, *JHEP* **02**, 097 (2016), [arXiv:1511.05162 \[hep-ph\]](#).
- [14] L. Wang and X.-F. Han, *JHEP* **05**, 039 (2015), [arXiv:1412.4874 \[hep-ph\]](#).
- [15] T. Abe, R. Sato, and K. Yagyu, *JHEP* **07**, 064 (2015), [arXiv:1504.07059 \[hep-ph\]](#).
- [16] A. Crivellin, J. Heeck, and P. Stoffer, *Phys. Rev. Lett.* **116**, 081801 (2016), [arXiv:1507.07567 \[hep-ph\]](#).
- [17] E. J. Chun and J. Kim, *JHEP* **07**, 110 (2016), [arXiv:1605.06298 \[hep-ph\]](#).
- [18] V. Ilisie, *JHEP* **04**, 077 (2015), [arXiv:1502.04199 \[hep-ph\]](#).
- [19] A. Cherchiglia, D. Stöckinger, and H. Stöckinger-Kim, *EPJ Web Conf.* **179**, 01022 (2018).
- [20] A. S. de Jesus, S. Kovalenko, F. S. Queiroz, C. A. de S. Pires, and Y. S. Villamizar, *Phys. Lett. B* **809**, 135689 (2020), [arXiv:2003.06440 \[hep-ph\]](#).
- [21] A. Doff and C. A. d. S. Pires, (2024), [arXiv:2403.19338 \[hep-ph\]](#).
- [22] T. T. Hong, L. T. T. Phuong, T. P. Nguyen, N. H. T. Nha, and L. T. Hue, (2024), [arXiv:2404.05524 \[hep-ph\]](#).
- [23] J. a. P. Pinheiro, C. A. de S. Pires, F. S. Queiroz, and Y. S. Villamizar, *Phys. Lett. B* **823**, 136764 (2021), [arXiv:2107.01315 \[hep-ph\]](#).
- [24] C. Kelso, H. N. Long, R. Martinez, and F. S. Queiroz, *Phys. Rev. D* **90**, 113011 (2014), [arXiv:1408.6203 \[hep-ph\]](#).
- [25] N. A. Ky, H. N. Long, and D. Van Soa, *Phys. Lett. B* **486**, 140 (2000), [arXiv:hep-ph/0007010](#).
- [26] A. E. Cárcamo Hernández, Y. Hidalgo Velásquez, S. Kovalenko, H. N. Long, N. A. Pérez-Julve, and V. V. Vien, *Eur. Phys. J. C* **81**, 191 (2021), [arXiv:2002.07347 \[hep-ph\]](#).
- [27] R. Foot, H. N. Long, and T. A. Tran, *Phys. Rev. D* **50**, R34 (1994), [arXiv:hep-ph/9402243](#).
- [28] J. C. Montero, F. Pisano, and V. Pleitez, *Phys. Rev. D* **47**, 2918 (1993), [arXiv:hep-ph/9212271](#).
- [29] J. P. Pinheiro and C. A. de S. Pires, *Phys. Lett. B* **836**, 137584 (2023), [arXiv:2210.05426 \[hep-ph\]](#).
- [30] V. Oliveira and C. A. d. S. Pires, *J. Phys. G* **50**, 115002 (2023), [arXiv:2208.00420 \[hep-ph\]](#).

- [31] V. Oliveira and C. A. de S. Pires, *Phys. Lett. B* **846**, 138216 (2023), [arXiv:2211.03835 \[hep-ph\]](#).
- [32] H. N. Long, *Phys. Rev. D* **54**, 4691 (1996), [arXiv:hep-ph/9607439](#).
- [33] H. N. Long, *Mod. Phys. Lett. A* **13**, 1865 (1998), [arXiv:hep-ph/9711204](#).
- [34] H. N. Long, *Phys. Rev. D* **53**, 437 (1996), [arXiv:hep-ph/9504274](#).
- [35] H. N. Long and D. V. Soa, in 32nd Rencontres de Moriond: Electroweak Interactions and Unified Theories (1997) pp. 249–255.
- [36] Q.-H. Cao and D.-M. Zhang, (2016), [arXiv:1611.09337 \[hep-ph\]](#).
- [37] C. A. de S. Pires and P. S. Rodrigues da Silva, *Eur. Phys. J. C* **36**, 397 (2004), [arXiv:hep-ph/0307253](#).
- [38] Y. A. Coutinho, V. Salustino Guimarães, and A. A. Nepomuceno, *Phys. Rev. D* **87**, 115014 (2013), [arXiv:1304.7907 \[hep-ph\]](#).
- [39] A. Alves, L. Duarte, S. Kovalenko, Y. M. Oviedo-Torres, F. S. Queiroz, and Y. S. Villamizar, *Phys. Rev. D* **106**, 055027 (2022), [arXiv:2203.02520 \[hep-ph\]](#).
- [40] A. Doff, C. A. de S. Pires, and P. S. R. da Silva, *Phys. Rev. D* **74**, 015014 (2006), [arXiv:hep-ph/0604021](#).
- [41] A. L. Cherchiglia and O. L. G. Peres, *JHEP* **04**, 017 (2023), [arXiv:2209.12063 \[hep-ph\]](#).
- [42] Z. Fan and K. Yagyu, *JHEP* **06**, 014 (2022), [arXiv:2201.11277 \[hep-ph\]](#).
- [43] H. Okada, N. Okada, Y. Orikasa, and K. Yagyu, *Phys. Rev. D* **94**, 015002 (2016), [arXiv:1604.01948 \[hep-ph\]](#).
- [44] M. Lindner, M. Platscher, and F. S. Queiroz, *Phys. Rept.* **731**, 1 (2018), [arXiv:1610.06587 \[hep-ph\]](#).
- [45] A. Cherchiglia, P. Kneschke, D. Stöckinger, and H. Stöckinger-Kim, *JHEP* **01**, 007 (2017), [Erratum: *JHEP* **10**, 242 (2021)], [arXiv:1607.06292 \[hep-ph\]](#).
- [46] D. Chang, W.-F. Chang, C.-H. Chou, and W.-Y. Keung, *Phys. Rev. D* **63**, 091301 (2001), [arXiv:hep-ph/0009292](#).
- [47] E. J. Chun, J. Kim, and T. Mondal, *JHEP* **12**, 068 (2019), [arXiv:1906.00612 \[hep-ph\]](#).
- [48] P. M. Ferreira, B. L. Gonçalves, F. R. Joaquim, and M. Sher, *Phys. Rev. D* **104**, 053008 (2021), [arXiv:2104.03367 \[hep-ph\]](#).
- [49] C. Promberger, S. Schatt, and F. Schwab, *Phys. Rev. D* **75**, 115007 (2007), [arXiv:hep-ph/0702169](#).
- [50] R. H. Benavides, Y. Giraldo, and W. A. Ponce, *Phys. Rev. D* **80**, 113009 (2009), [arXiv:0911.3568 \[hep-ph\]](#).
- [51] A. J. Buras, F. De Fazio, J. Gierbach, and M. V. Carlucci, *JHEP* **02**, 023 (2013), [arXiv:1211.1237 \[hep-ph\]](#).

- [52] A. J. Buras, F. De Fazio, and J. Girrbach, *JHEP* **02**, 112 (2014), arXiv:1311.6729 [hep-ph].
- [53] A. J. Buras and F. De Fazio, *JHEP* **03**, 219 (2023), arXiv:2301.02649 [hep-ph].
- [54] D. Nguyen Tuan, T. Inami, and H. Do Thi, *Eur. Phys. J. C* **81**, 813 (2021), arXiv:2009.09698 [hep-ph].
- [55] D. Cogollo, A. V. de Andrade, F. S. Queiroz, and P. Rebello Teles, *Eur. Phys. J. C* **72**, 2029 (2012), arXiv:1201.1268 [hep-ph].
- [56] F. S. Queiroz, C. Siqueira, and J. W. F. Valle, *Phys. Lett. B* **763**, 269 (2016), arXiv:1608.07295 [hep-ph].
- [57] A. E. Cárcamo Hernández, L. Duarte, A. S. de Jesus, S. Kovalenko, F. S. Queiroz, C. Siqueira, Y. M. Oviedo-Torres, and Y. Villamizar, *Phys. Rev. D* **107**, 063005 (2023), arXiv:2208.08462 [hep-ph].
- [58] G. Buchalla, A. J. Buras, and M. E. Lautenbacher, *Rev. Mod. Phys.* **68**, 1125 (1996), arXiv:hep-ph/9512380.
- [59] L. Di Luzio, M. Kirk, A. Lenz, and T. Rauh, *JHEP* **12**, 009 (2019), arXiv:1909.11087 [hep-ph].
- [60] K. De Bruyn, R. Fleischer, E. Malami, and P. van Vliet, *J. Phys. G* **50**, 045003 (2023), arXiv:2208.14910 [hep-ph].
- [61] B. Wang, *PoS LATTICE2019*, 093 (2019), arXiv:2001.06374 [hep-lat].
- [62] B. Wang, *PoS LATTICE2021*, 141 (2022).
- [63] O. Deschamps, S. Descotes-Genon, S. Monteil, V. Niess, S. T'Jampens, and V. Tisserand, *Phys. Rev. D* **82**, 073012 (2010), arXiv:0907.5135 [hep-ph].
- [64] D. Chowdhury and O. Eberhardt, *JHEP* **05**, 161 (2018), arXiv:1711.02095 [hep-ph].
- [65] P. Arnan, D. Bečirević, F. Mescia, and O. Sumensari, *Eur. Phys. J. C* **77**, 796 (2017), arXiv:1703.03426 [hep-ph].
- [66] M. Aoki, S. Kanemura, K. Tsumura, and K. Yagyu, *Physical Review D* **80**, 015017 (2009).
- [67] F. Mahmoudi and O. Stal, *Physical Review D* **81**, 035016 (2010).
- [68] M. Jung, A. Pich, and P. Tuzon, *European Physical Journal C* **74**, 268 (2014).
- [69] A. J. Buras and F. De Fazio, *JHEP* **08**, 115 (2016), arXiv:1604.02344 [hep-ph].
- [70] A. J. Buras, P. Colangelo, F. De Fazio, and F. Loparco, *JHEP* **10**, 021 (2021), arXiv:2107.10866 [hep-ph].
- [71] M. S. Lang and U. Nierste, *JHEP* **04**, 047 (2024), arXiv:2212.11086 [hep-ph].
- [72] Y. S. Amhis et al. (HFLAV), *Phys. Rev. D* **107**, 052008 (2023), arXiv:2206.07501 [hep-ex].
- [73] D. Das, *Int. J. Mod. Phys. A* **30**, 1550158 (2015), arXiv:1501.02610 [hep-ph].
- [74] F. Borzumati and C. Greub, in *29th International Conference on High-Energy Physics* (1998) pp.

- 1735–1739, [arXiv:hep-ph/9810240](#).
- [75] M. Ciuchini, G. Degrossi, P. Gambino, and G. F. Giudice, *Nucl. Phys. B* **527**, 21 (1998), [arXiv:hep-ph/9710335](#).
- [76] A. Arbey, F. Mahmoudi, O. Stal, and T. Stefaniak, *Eur. Phys. J. C* **78**, 182 (2018), [arXiv:1706.07414 \[hep-ph\]](#).
- [77] O. Atkinson, M. Black, A. Lenz, A. Rusov, and J. Wynne, *JHEP* **04**, 172 (2022), [arXiv:2107.05650 \[hep-ph\]](#).
- [78] T. Enomoto and R. Watanabe, *JHEP* **05**, 002 (2016), [arXiv:1511.05066 \[hep-ph\]](#).
- [79] M. Misiak, A. Rehman, and M. Steinhauser, *JHEP* **06**, 175 (2020), [arXiv:2002.01548 \[hep-ph\]](#).
- [80] G. C. Branco, P. M. Ferreira, L. Lavoura, M. N. Rebelo, M. Sher, and J. P. Silva, *Phys. Rept.* **516**, 1 (2012), [arXiv:1106.0034 \[hep-ph\]](#).
- [81] H. E. Haber and D. O’Neil, *Physical Review D* **83**, 055017 (2011).
- [82] P. B. Pal, *Phys. Rev. D* **52**, 1659 (1995), [arXiv:hep-ph/9411406](#).
- [83] A. Barroso, P. M. Ferreira, I. P. Ivanov, and R. Santos, *JHEP* **06**, 045 (2013), [arXiv:1303.5098 \[hep-ph\]](#).
- [84] I. F. Ginzburg and I. P. Ivanov, *Phys. Rev. D* **72**, 115010 (2005), [arXiv:hep-ph/0508020](#).
- [85] N. Chen, T. Han, S. Su, W. Su, and Y. Wu, *JHEP* **03**, 023 (2019), [arXiv:1808.02037 \[hep-ph\]](#).
- [86] T. Han, S. Li, S. Su, W. Su, and Y. Wu, *JHEP* **01**, 045 (2021), [arXiv:2008.05492 \[hep-ph\]](#).